Minimal Heating at the Skin Surface During Transcranial Direct Current Stimulation

Niranjan Khadka, PhD Candidate; Adantchede L. Zannou, BS; Fatima Zunara, BS; Dennis Q. Truong, PhD Candidate; Jacek Dmochowski, PhD; Marom Bikson, PhD

Objective: To assess if transcranial direct current stimulation (tDCS) produces a temperature change at the skin surface, if any change is stimulation polarity (anode or cathode) specific, and the contribution of passive heating (joule heat) or blood flow on such change.

Material and Methods: Temperature differences (ΔTs) in an agar phantom study and an *in vivo* study (forearm stimulation) including 20 volunteers with both experimental measures and finite element method (FEM) multiphysics prediction (current flow and bioheat) models of skin comprising three tissue layers (epidermis, dermis, and subcutaneous layer with blood perfusion) or of the phantom for active stimulation and control cases were compared. Temperature was measured during pre, post, and stimulation phases for both phantom and subject's forearms using thermocouples.

Results: In the phantom, ΔT under both anode and cathode, compared to control, was not significantly different and less than 0.1°C. Stimulation of subjects resulted in a gradual increase in temperature under both anode and cathode electrodes, compared to control (at $t = 20$ min: ΔTanode = 0.9°C, ΔTcathode = 1.1°C, ΔTcontrol = 0.05°C). The FEM phantom model predicted comparable maximum ΔT of 0.27°C and 0.28°C (at $t = 20$ min) for the control and anode/cathode cases, respectively. The FEM skin model predicted a maximum ΔT at $t = 20$ min of 0.98°C for control and 1.36°C under anode/cathode electrodes.

Conclusions: Taken together, our results indicate a moderate and nonhazardous increase in temperature at the skin surface during 2 mA tDCS that is independent of polarity, and results from stimulation induced blood flow rather than joule heat.

Keywords: bioheat, erythema, finite element method, flare, transcranial direct current stimulation, temperature, passive heating (joule heat), skin

Conflict of Interest: Marom Bikson received grants from NIH. The City University of New York (CUNY) has IP on neuro-stimulation system and methods with author, Niranjan Khadka and other coauthors, Jacek Dmochowski and Marom Bikson as inventors. Dr. Marom Bikson has equity in Soterix Medical Inc.

INTRODUCTION

Transcranial direct current stimulation (tDCS) is investigated as a noninvasive neuromodulation tool in healthy and patient populations (1). Transient cutaneous sensation (e.g., itching, tingling, warmth) and skin erythema (so called "flare") are the primary reported side effects of tDCS (2). Only using nonoptimal materials and procedures can more severe skin irritation be observed (3,4). These adverse skin responses can be minimized by following established protocols in dose and electrode preparation (5,6), monitoring electrode resistance (7,8), and using proven electrode designs (6,9) or more advanced electrode techniques (10,11).

One of the concerns to be addressed during the tDCS stimulation is the change in temperature at the skin surface. These changes might be stimulation polarity (anode or cathode) specific, contributed due to passive heating (joule heat), or due to change in blood perfusion. Small noninjurious changes in skin temperature during tDCS may influence cutaneous sensation (12) and even influence current flow patterns to the brain (13,14). Such changes may also confound blinding of subjects (e.g., sensation of warmth that is based on real temperature changes) or operators (e.g., in the active case sponges are warmer). Although higher temperature changes may be injurious and

contribute to less tolerable treatment, prior experimental, and finite element method (FEM) modeling studies have curtailed a role for significant temperature increases during tDCS (15,16).

This study also builds upon the prior study by Datta et al., where no significant temperature rise at the sponge- electrode and the scalp interface was predicted by the FEM simulation of 2 mA 4 × 1

Address correspondence to: Niranjan Khadka, PhD Candidate, or Marom Bikson, PhD, Department of Biomedical Engineering, The City College of New York, CUNY, New York, NY, USA. Email: nkhadka@ccny.cuny.edu; bikson@ccny.cuny.edu

Department of Biomedical Engineering, The City College of New York, CUNY, New York, NY USA

[Correction added on 14 February 2017, after first online publication: The third author's name has been corrected from "Fatima Zunura" to "Fatima Zunara".]

ring HD-tDCS and conventional tDCS. Here, using an array of precise thermocouples, we measured temperature changes at the electrode-sponge and the agar phantom interface, and the skin interface, on an easily accessible area of skin such as forearms, during anodal, cathodal, and sham stimulation. Though systemic (centrally mediated) temperature changes during tDCS have not been observed (17), we none-the-less stimulated subjects' forearms to remove a central confound. As a first demonstration, we implemented detailed experimental measures along with computational FEM model of an agar phantom (control experiment where vasculature is absent) and a skin [that included a vascular flare response (18–20)] to determine the role of joule heating vs. vascular flare (explained in discussion section) on any temperature changes.

MATERIALS AND METHODS

This study involves experimental measurements in phantom and participant, and FEM simulation for stimulation (anode or cathode) and control cases.

Participants

Twenty healthy subjects (14 males and 6 females; age range 20–30 years; mean age 23.5 ± 2.5) volunteered in the study. Participants with any form of skin disorders or preexisting injuries at the sites of stimulation were excluded. The CCNY local Ethics Committee granted approval for this study and a written informed consent from the participants was collected before conducting the experiment. Participants were seated in a relaxed position.

Stimulation and Temperature Measurement

A constant current stimulator (1 × 1 tDCS, Soterix Medical Inc., NY, USA) was used to administer direct current for all trials through a pair of rubber electrodes (2 × 3 cm) placed into two saline (0.9% NaCl) soaked sponge pockets (35 cm^2 skin contact area, EasyPads, Soterix Medical Inc., NY, USA). Direct current intensity of 2 mA was applied for 20 min with an additional linear ramp up and down of 30 sec at the beginning and at the end of stimulation. Six type- K thermocouples probes (Digi-Key Electronics, MN, USA) sensed by three dual input digital thermometers (∼ ± [0.05% of reading + 0.3°C] accuracy, 52II, Fluke Corporation, WA, USA) were positioned under the center and periphery of the anode, cathode, and control sponge-electrode to measure the temperature during stimulation (anode, cathode) and control (nonstimulation) electrode cases. Temperature was measured during stimulation (20 min), and prestimulation and poststimulation (5 min each) phases for every minute. Measurement of temperature under the anode, cathode, and control was conducted during the same stimulation session—with the control electrode positioned on the opposite arm or at a distance location on the phantom. Experiments were conducted at the bench top in a temperature-controlled room and the ambient temperature was continuously monitored during the experiment using two similar type- K thermocouples as mentioned above. The ambient room temperature during the entire study remained nearly unchanged (22 ± 1.5°C).

Phantom Study

Agar *phantom* (2% agar by weight; 20 gm agar ash, and 1 gm NaCl to 1000 mL water, A7002, Sigma-Aldrich, MO, USA) was prepared using established standard protocols (21). While conducting temperature measurement on the phantom, sponge-electrodes were positioned approximately 10.2 cm apart on a thin coated layer (∼0.5 cm) of conductive electrode gel (Signa gel, Parker Laboratories Inc., NJ, USA). Assigned electrode distance was based on our earlier study (8). The electrode-sponge distance in the phantom study matched the *in vivo* study. Conductive gel layer was used to maintain consistent contact between the sponge-electrode and the gel. For stimulation case, a 2 mA DC was injected from the 1 × 1 tDCS stimulator via sponge electrodes and corresponding temperature under the electrodes were measured whereas for the control case, sponge electrodes were positioned on the phantom but not connected to the stimulator.

In Vivo Study

For *in vivo* study, skin was cleaned with dilute saline prior to the electrode placement. The sponge electrodes were then secured on the forearm of the participants using rubber straps (Elastic Fasteners "Blue," Soterix Medical Inc., NY, USA) and were positioned proximal and distal to the forearm (8). Stimulation and control cases, and the corresponding temperature measurement were conducted following the aforementioned procedure.

Temperature Analysis

Temperature measurements at every minute during prestimulation, stimulation, and poststimulation phases for both phantom and *in vivo* studies were averaged across phantoms and subjects, and were normalized with respect to the initial temperature, which was considered a baseline (0°C) as shown in Figure 1a. Since the initial temperature on the placement of the sponge-electrodes at the skin or the phantom varied with the initial temperature of the saline soaked sponges and the ambient temperature, we considered initiation of the tDCS stimulation ($t = 5$ min) as the "initial temperature" for normalizing temperature data. Temperature difference (ΔT) was calculated across all subjects and phantom studies for both stimulation and control cases. In case of the FEM simulations, ΔT was calculated at the given instant ($t = 5, 10, 15,$ and 20 min).

Computational Model and Solution Method

Heat Transfer

Human skin was modeled as an inhomogeneous medium comprising three layers; epidermis, dermis, and subcutaneous layer (fat and connective tissue) where epidermis was superficial and avascular (presence of stratum corneum [SC]), while the underlying dermis and subdermal tissues were rich in vasculature (22,23). Each layer of the skin was modeled as a homogeneous and isotropic volume conductor and thickness values were based from prior literature (23). The anodal case was considered for the FEM multiphysics (current flow and bioheat) model, however, none of the physics considered for the computational model were polarity specific. Heat transfer and temperature fields in the human skin was modeled using time-dependent bioheat equation Pennes equation as mentioned below:

$$\rho C_p \nabla T = \nabla . (\kappa \nabla T) - \rho_b C_b \omega_b (T - T_b) + Q_{met} \quad (1)$$

where ρ, C_p, T, κ, and Q_{met} represent tissue density, specific heat, temperature, thermal conductivity, and metabolic heat generation, respectively. Similarly, ρ_b, C_b, ω_b, and T_b are density of the blood, specific heat of the blood, blood perfusion rate, and temperature of arterial blood. Blood perfusion was constant in all vascular skin layers and the values for the properties of blood were assigned as: $\rho_b = 1060$ kg/m^3(24); $C_b = 3770$ J/(kg.K); $T_b = 37°C$ (25). In order to account for the heat generation during electrical stimulation, equation (1) was further modified to include joule heating
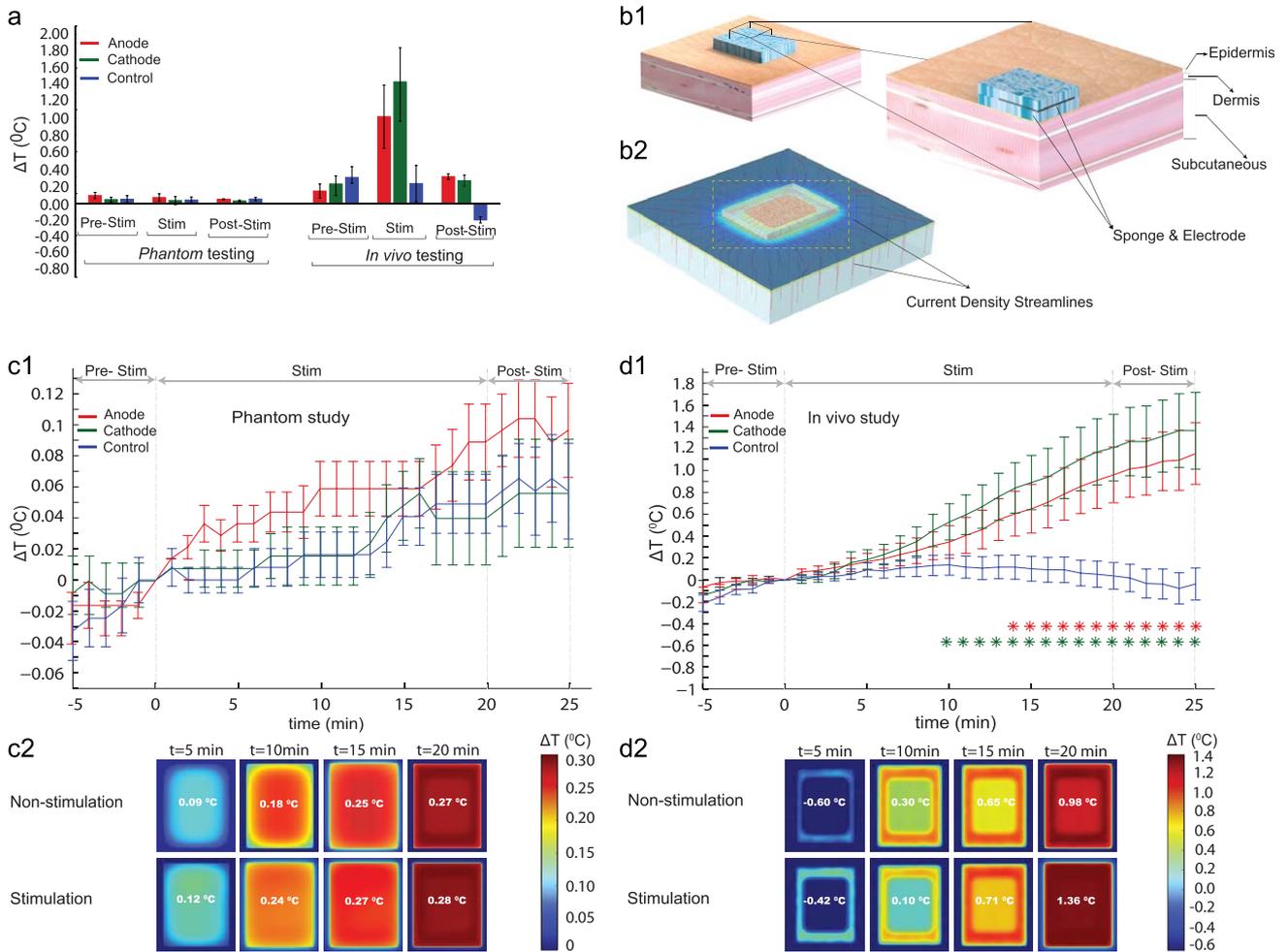
Figure 1. Skin surface temperature changes under tDCS electrodes during prestimulation, stimulation, and poststimulation phases in the phantom from *in vivo* studies, and FEM simulations. a Average temperature change in subjects (right) and phantom (left) normalized to temperature at $t = 0$. The error bars indicate standard error of mean. In the phantom, ΔT was approximately same across test samples and mode of stimulation, whereas in the *in vivo* study, maximum ΔT was measured under the active electrode (max. under cathode) during stimulation compared to the control. b1 Architecture of a skin model showing skin layers (epidermis, dermis, and subcutaneous layers) and electrode positioning on the skin surface. b2 represents an orientation of current density flow streamlines inside the different skin tissue layers. c1 Analysis of normalized average ΔT in the phantom study ($p < 0.01$). No significant difference in ΔT was found in the control, compared to the anode and the cathode. c2 Illustration of predicted ΔT for the nonstimulation (control) and stimulation cases in the FEM phantom model. Predicted results indicated no significant effect of stimulation on the phantom. d1 *In vivo* analysis of temperature difference over time within subjects during prestimulation, stimulation, and poststimulation. Red and green asterisks symbolize statistical significant difference ($p < 0.01$) between anode and control, and cathode and control, respectively. There was a significant difference in ΔT under the anode ($p < 0.01$) and the cathode ($p < 0.01$), compared to the control. Temperature under both anode and cathode gradually increased due to stimulation, compared to that of control. d2 FEM representation of the predicted ΔT in the skin model. Maximum ΔT of 1.36°C was predicted during direct current stimulation by the FEM model.

(Laplace equation $\nabla(\sigma\nabla V)=0$ where V: potential and σ: conductivity) and was given by:

$$\rho C_p\nabla T=\nabla.(\kappa\nabla T)-\rho_b C_b\omega_b(T-T_b)+Q_{met}+\sigma|\nabla V^2| \quad (2)$$

Boundary and Initial Conditions

The boundary condition at the top surface of the skin and sponge was simulated as convective heat loss to the ambient air, without explicitly considering heat loss to the surrounding due to evaporation. Therefore, the boundary conditions at the top surface of the skin and sponge electrode was

$$q=h(T_{amb}-T)$$
$$h = 5 \text{ W/m}^2\text{.K}, \quad T_{amb} = 24°C \text{ (air temperature)} \quad (3)$$

where h is the convective heat transfer coefficient and T_{amb} was ambient temperature (averaged from *in vivo* study). Bottom surface

of subcutaneous layer was set to be at core temperature (T_{core}) and the boundary condition was ($T_{core} = 37°C$).

Initial temperatures (T_0) for electrode-sponge (22.5°C), top layer of skin (surrounding epidermis = 32.5°C, and epidermis section underpad = 29.02°C) were based on experimental measurement. The underlying dermis (33°C) and subcutaneous layer (33°C) temperature was set slightly higher than the epidermis due to vasculature and proximity to the core (23).

For electrical stimulation, boundary conditions were applied as normal current density (inward current flow:J_{norm}) at the top exposed surface of anode and ground at the bottom surface of subcutaneous layer. Uniform current density corresponding to 2 mA intensity was applied through a rubber electrode [$\sigma = 0.947$ S/m; $\kappa = 0.2$ W/(m.K),(26)], embedded inside sponge pocket [$\sigma = 1.4$ S/m; $\kappa = 0.6$ W/(m.K), (27)]. All other external surfaces of the model were electrically insulated. Dimensions of rubber electrode and sponge were set according to the experimental protocol.

The thermophysical parameters of biological tissue layers were based on average of prior literature (23–25,28,29). Epidermis under the wet sponge [$\sigma = 0.16$ S/m; $\kappa = 0.235$ W/(m.K)] was assigned higher conductivity compared to the surrounding dry epidermis [$\sigma = 0.0004$ S/m; $\kappa = 0.235$ W/(m.K)] due to the water content in the saline. Blood perfusion in the vascular tissues was increased with current density, simulating stimulation-induced erythema (flare response). Dermis ($\sigma = 0.23$ S/m; $\kappa = 0.450$ W/(m.K), $\omega_b = 0.0020$ s^{-1}, $Q_{met} = 400$ Wm^{-3}), and subcutaneous layer ($\sigma = 0.02$ S/m; $\kappa = 0.185$ W/(m.K), $\omega_b = 0.001$ s^{-1}, $Q_{met} = 400$ Wm^{-3}) have blood perfusion due to vasculature, hence metabolic heat generation.

The phantom was modeled using equations (1) and (2) neglecting the biological tissue parameters. The boundary and initial temperatures of the phantom were set based on experimental measurement ($T_{core} = T_0 = 24°C$). The electrical conductivity and thermal conductivity of agar phantom were 0.05 S/m and 0.07 W/(m.K), respectively (30).

Computational Method

Computer aided design models of skin layer geometry consisting epidermis, dermis, subcutaneous layer, sponge, and electrode (Fig. 1b1) were assembled in SolidWorks 2013 (Dassault Systemes Americas Corp., MA, USA) and were imported as an assembly in COMSOL Multiphysics 4.3 (COMSOL Inc., MA, USA) to solve the model using a finite element technique. The phantom model was solved implementing the same methods as the skin model. Volumetric meshes for the skin and the phantom model were generated as *Physic-controlled mesh* with an average element quality of greater than 0.5. The final FEM skin model was solved for greater than 2,000,000 degrees of freedom and had greater than 1,700,000 tetrahedral elements whereas in the phantom model, the degrees of freedom was greater 600,000 and had greater than 400,000 tetrahedral elements. In our study, we considered the steady-state solution (temperature obtained by evaluating the model under nonstimulation condition) as the initial conditions for the time-dependent study (20 min stimulation with a time step of 0.01 sec) of temperature elevation. Bio-heat transfer physics in biological tissues (for the skin) and solid (for the phantom) were solved for stimulation and nonstimulation cases and the temperature were predicted. Current density streamlines were generated for the stimulation case (skin) to illustrate the distribution of current on the surface and through different tissue layers (Fig. 1b2). Streamlines were seeded uniformly from the top surface of the rubber electrode and were proportional to the logarithm of current density magnitude.

Datasets from the computational result of the skin and the phantom volume plots (non-stimulation and stimulation cases) were exported from COMSOL and were analyzed in MATLAB R2016a (MathWorks, MA, USA) to calculate the temperature difference (ΔT). Since the FEM model was first solved under steady-state condition and later its solutions were used as the initial conditions for the time-dependent study, we considered temperature at $t = 1$ min as the initial temperature for the ΔT computation of both phantom and skin model.

Statistical Analysis

Analyses were performed using Shapiro-Wilk test to access normality of temperature difference across active stimulation (anodal, cathodal) and control groups. Statistically significant differences ($p < 0.01$) in ΔT between polarities (anode, cathode, and control) were probed using a nonparametric analysis. Specifically, Friedman's test was conducted to evaluate differences in ΔT among each group—when significant, a post hoc analysis (corrected multiple comparisons) was performed using Dunn's test. A critical value of less than 0.01 was accepted as a significant difference between the groups.

RESULTS

Temperature changes at the skin surfaced under electrodes during active direct current stimulation (2 mA, 20 min) and control (0 mA, 20 min) conditions were recorded on subject forearms and a specially constructed phantom. Additionally, temperature increases were also simulated using bio-heat FEM models of the skin and phantom surface. In both phantom and subjects, we observed a dynamic temperature variation reflecting difference in the initial temperature at the skin electrode interface when the sponges were initially placed on the forearm at a given ambient room temperature in all cases. Therefore, all analysis was performed relative to the temperature at the surface of the skin, 5 min after the sponge was initially placed; corresponding to when stimulation was initiated in the active stimulation case (Fig. 1c1 and 1d1).

Average temperature difference (ΔT) across stimulation group and control in the phantom was less than 0.1°C (Fig. 1a). ΔT was not significantly different under both anode (Mdn = 0.0687°C) and cathode (Mdn = 0.046°C), compared to control (Mdn = 0.0260°C) (χ^2 (2, $N = 30$) = 0.27, $p > 0.01$, Fig. 1c1).

Stimulation of subjects resulted in a gradual increase in temperature under both anode and cathode, compared to control (e.g., at $t = 20$ min: ΔTanode = 0.9°C, ΔTcathode = 1.1°C, ΔTcontrol = 0.05°C as shown in Fig. 1d1). We found a main effect of stimulation type (anode, cathode, or control) on ΔT (Friedman's test, χ^2 (2, $N = 30$) = 64.13, $p < 0.01$). Further pairwise comparison using Dunn's test indicated a lower ΔT in control compared to both anode ($Z = -2.389$, $p < 0.01$) and cathode ($Z = -2.6133$, $p < 0.01$). However, the median ΔT between anode and cathode was not significantly different ($Z = -0.5973$, $p > 0.01$).

The FEM model of stimulation on the skin and phantom predicted current flow pattern produced across the tissue/phantom (Fig. 1b2) and the coupled change in heat and blood flow (for the case of the skin). The phantom FEM model predicted a comparable maximum ΔT of 0.27°C and 0.28°C (at $t = 20$ min) for the nonstimulation (control) and stimulation (anode/cathode) cases, respectively (Fig. 1c2). A maximum ΔT of 0.98°C was predicated by the FEM skin model at $t = 20$ min for the nonstimulation case, whereas for the stimulation case, ΔT was 1.36°C (Fig. 1d2). Compared to the control case, tDCS induced a moderate temperature rise ($\Delta T = 0.38°C$) at the skin surface, as predicted by the FEM skin model ($t = 20$ min).

DISCUSSION

Any electrical stimulation might produce temperature changes; reflecting complex interactions between joule heat due to applied current across resistive tissue, changes in metabolism (neuronal activation) or perfusion (flare), and heat conduction (31,32). Evidently, the results of our study are relevant only for the specific technology, dose, and subject conditions tested [c.f., transcranial magnetic stimulation in the presence of a heating clip (33)]. Temperature changes in the body are typically considered unimportant in the efficacy or safety of neuromodulation technologies (34,35). We observed only incremental temperature changes at the skin surface during tDCS, independent of stimulation polarity and results from stimulation.

Since changes were absent in the phantom, we propose that temperature elevation increases the anode/cathode reflected stimulation induced flare—a heating induced skin response due to increased blood flow. Skin surface temperature changes of ~1°C are none injurious and within normal variation [e.g., due to exercise, environment; (31,36)]. Moreover, as this small increment is in fact compensating for a reduction in surface temperature following application of room-temperature sponges, and since the core body temperature of the blood limits perfusion-based heating, this mechanism is not hazardous.

Our results are consistent with the tDCS perception of warmth being attributed to electrical nerve activation rather than heating (32,35), and any significant skin irritation (that occurs only when standard protocols are not followed) being electrochemical in nature (37). We analyzed temperature change at the surface of the skin (in vivo study) during stimulation (20 min) relative to the temperature after the prestimulation duration (5 min) to account for the dynamic temperature changes reflecting difference in the initial temperature at the skin-electrode interface relative to the skin and room temperature (Fig. 1d1). Similarly, to account for such dynamic temperature variation due to natural cooling of the skin when exposed to the ambient temperature, we solved our FEM models first under steady-state conditions and then used its solution as an initial condition for the time-dependent analysis. Any warming of sponges observed by subjects or operators touching the electrode surface would reflect passive heating from the body and it is unlikely that the difference between active and sham can be resolved, hence, not a confound to blinding. Our result does not address temperature changes inside the body (e.g., at the brain), temperature changes outside of the period evaluated (up to 5 min post tDCS), microscopic changes (e.g., at sweat pores) or changes following abnormal tDCS dose (e.g., 100 mA), and repeated sessions. We speculate the flare response, already a well-known consequence of tDCS from inspection of skin erythema (20,38), along with the associated skin temperature change indicated here, may influence current flow patterns through the skin, and so indirectly tolerability (39). For future research, this approach can be extended to a realistic head model or a microscopic level skin model.

Authorship Statements

Niranjan Khadka, Adantchede L. Zannou, and Fatima Zunura designed and conducted this study, including data collection, subject recruitment, and data analysis. Dr. Marom Bikson supervised the entire study. Dr. Jacek Dmochowski oversaw the data analysis. Dennis Troung revised the draft.

REFERENCES

1. Nitsche MA, Paulus W. Excitability changes induced in the human motor cortex by weak transcranial direct current stimulation. J Physiol 2000;527:633–639.
2. Nitsche MA, Cohen LG, Wassermann EM et al. Transcranial direct current stimulation: state of the art 2008. Brain Stimul 2008;1:206–223.
3. Poreisz C, Boros K, Antal A, Paulus W. Safety aspects of transcranial direct current stimulation concerning healthy subjects and patients. Brain Res Bull 2007;72:208–214.
4. Bikson M, Datta A, Elwassif M. Establishing safety limits for transcranial direct current stimulation. Clin Neurophysiol 2009;120:1033–1034.
5. Brunoni AR, Nitsche MA, Bolognini N et al. Clinical research with transcranial direct current stimulation (tDCS): challenges and future directions. Brain Stimul 2012;5:175–195.
6. Woods AJ, Antal A, Bikson M et al. A technical guide to tDCS, and related non-invasive brain stimulation tools. Clin Neurophysiol 2016;127:1031–1048.
7. Merrill DR, Bikson M, Jefferys JGR. Electrical stimulation of excitable tissue: design of efficacious and safe protocols. J Neurosci Methods 2005;141:171–198.
8. Khadka N, Rahman A, Sarantos C, Truong DQ, Bikson M. Methods for specific electrode resistance measurement during transcranial direct current stimulation. Brain Stimul 2015;8:150–159.
9. Brunoni AR, Amadera J, Berbel B, Volz MS, Rizzerio BG, Fregni F. A systematic review on reporting and assessment of adverse effects associated with transcranial direct current stimulation. Int J Neuropsychopharmacol 2011;14:1133–1145.
10. Khadka N, Truong DQ, Bikson M. Principles of within electrode current steering. J Med Devices 2015;9:020947–020947.
11. Kempe R, Huang Y, Parra LC. Simulating pad-electrodes with high-definition arrays in transcranial electric stimulation. J Neural Eng 2014;11:26003.
12. Lagopoulos J, Degabriele R. Feeling the heat: the electrode–skin interface during DCS. Acta Neuropsychiatr 2008;20:98–100.
13. Gholami-Boroujeny S, Mekonnen A, Batkin I, Bolic M. Theoretical analysis of the effect of temperature on current delivery to the brain during tDCS. Brain Stimul 2015;8:509–514.
14. DaSilva AF, Volz MS, Bikson M, Fregni F. Electrode Positioning and Montage in transcranial direct current stimulation. J Vis Exp 2011;(51). doi:10.3791/2744.
15. Palm U, Keeser D, Schiller C et al. Skin lesions after treatment with transcranial direct current stimulation (tDCS). Brain Stimul 2008;1:386–387.
16. Datta A, Elwassif M, Bikson M. Bio-heat transfer model of transcranial DC stimulation: comparison of conventional pad versus ring electrode. Conf Proc IEEE Eng Med Biol Soc 2009;2009:670–673.
17. Raimundo RJS, Uribe CE, Brasil-Neto JP. Lack of clinically detectable acute changes on autonomic or thermoregulatory functions in healthy subjects after transcranial direct current stimulation (tDCS). Brain Stimul 2012;5:196–200.
18. Dusch M, Schley M, Obreja O, Forsch E, Schmelz M, Rukwied R. Comparison of electrically induced flare response patterns in human and pig skin. Inflamm Res 2009;58:639–648.
19. Dusch M, Schley M, Rukwied R, Schmelz M. Rapid flare development evoked by current frequency-dependent stimulation analyzed by full-field laser perfusion imaging. Neuroreport 2007;18:1101–1105.
20. Guarienti F, Caumo W, Shiozawa P et al. Reducing transcranial direct current stimulation-induced erythema with skin pretreatment: considerations for sham-controlled clinical trials. Neuromodulation 2015;18:261–265.
21. Smith D. Agarose gel electrophoresis. In: Murphy D, Carter D, eds. Transgenesis techniques. Methods in Molecular BiologyTM. New York: Humana Press, 1993:433–438. http://dx.doi.org/10.1385/0-89603-245-0%3A433.
22. Hodson DA, Eason G, Barbenel JC. Modeling transient heat transfer through the skin and superficial tissues–1: surface insulation. J Biomech Eng 1986;108:183–188.
23. Wilson SB, Spence VA. A tissue heat transfer model for relating dynamic skin temperature changes to physiological parameters. Phys Med Biol 1988;33:895–912.
24. Duck FA, Physical properties of tissue: a comprehensive reference book. Cambridge, MA: Academic Press, 1990.
25. Torvi DA, Dale JD. A finite element model of skin subjected to a flash fire. J Biomech Eng 1994;116:250–255.
26. Khanam PN, Ponnamma D, AL-Madeed MA. Electrical properties of graphene polymer nanocomposites. In: Sadasivuni KK, Ponnamma D, Kim J, Thomas S, eds. Graphene-based polymer nanocomposites in electronics. Springer series on polymer and composite materials. Cham, Switzerland: Springer International Publishing, 2015:25–47.
27. Minhas P, Datta A, Bikson M. Cutaneous perception during tDCS: role of electrode shape and sponge salinity. Clin Neurophysiol 2011;122:637–638.
28. Werner J, Buse M. Temperature profiles with respect to inhomogeneity and geometry of the human body. J Appl Physiol 1988;65:1110–1118.
29. Pavselj N, Préat V, Miklavcic D. A numerical model of skin electropermeabilization based on in vivo experiments. Ann Biomed Eng 2007;35:2138–2144.
30. Bennett D. NaCl doping and the conductivity of agar phantoms. Mater Sci Eng C 2011;31:494–498.
31. Elwassif MM, Kong Q, Vazquez M, Bikson M, Bio-heat transfer model of deep brain stimulation induced temperature changes. Conf Proc IEEE Eng Med Biol Soc 2006;1:3580–3583.
32. Stephen AE, Caridad AB, Alan RC. Increased skin temperature during transcutaneous electrical stimulation. Anesth Analg 1980; 59:22–25.
33. Hsieh T-H, Dhamne SC, Chen J-JJ et al. Minimal heating of aneurysm clips during repetitive transcranial magnetic stimulation. Clin Neurophysiol 2012;123:1471–1473.
34. Balogun JA, Tang S, He Y, Hsieh JM, Katz JS. Effects of high-voltage galvanic stimulation of ST36 and ST37 acupuncture points on peripheral blood flow and skin temperature. Disabil Rehabil 1996;18:523–528.
35. Cramp G, Lowe W. The effect of high- and low-frequency transcutaneous electrical nerve stimulation upon cutaneous blood flow and skin temperature in healthy subjects. Clin Physiol 2000;20:150–157.

36. Scudds RJ, Helewa A, Scudds RA. The effects of transcutaneous electrical nerve stimulation on skin temperature in asymptomatic subjects. *Phys Ther* 1995;75:621–628.
37. Minhas P, Bansal V, Patel J et al. Electrodes for high-definition transcutaneous DC stimulation for applications in drug-delivery and electrotherapy, including tDCS. *J Neurosci Methods* 2010;190:188–197.
38. Ezquerro F, Moffa AH, Bikson M et al. The influence of skin redness on blinding in transcranial direct current stimulation studies: a crossover trial. *Neuromodulation* 2016; e-pub ahead of print. doi:10.1111/ner.12527

39. Khadka N, Seibt O, Patel V et al. Factors influencing current flow through the skin during transcranial electrical stimulation: role of waveform, tissue properties, and macro-pores. OASIS. 2015; http://www.abstractsonline.com/Plan/ViewAbstract.aspx?sKey=f764a1d5-9d4a-4eef-b8db-5ac9ba1bb047&cKey=30119eb6-1b29-428b-b7be-6487907aefdb&mKey=d0ff4555-8574-4fbb-b9d4-04eec8ba0c84.